# Journal of Materials Chemistry A

Accepted Manuscript


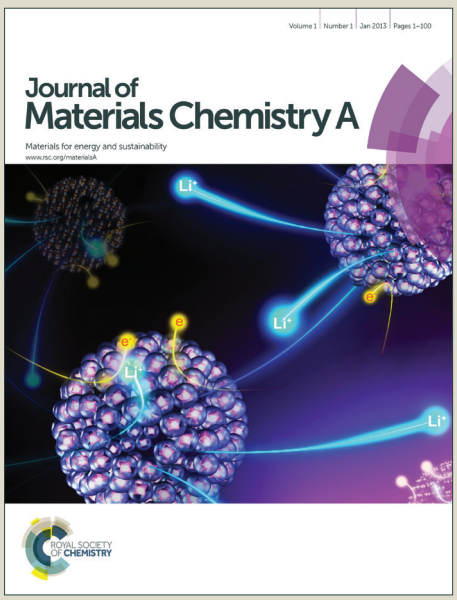





ROYAL SOCIETY OF CHEMISTRY

www.rsc.org/materialsA

Journal of
Materials Chemistry A

RSCPublishing

PAPER

# Novel diamine-modified composite nanofiltration membranes with chlorine resistance using monomers of 1,2,4,5-benzene tetracarbonyl chloride and m-phenylenediamine

Jinli Zhang, Yuyan Hai, Yi Zuo, Qian Jiang, Chang Shi, Wei Li*

Cite this: DOI: 10.1039/x0xx00000x

Novel polyamide thin film composite (TFC) nanofiltration (NF) membranes were prepared on polyetherimide supports by the interfacial polymerization of 1,2,4,5-benzene tetracarbonyl chloride and m-phenylenediamine followed by modification with ethylenediamine (EDA). The TFC NF membranes thus prepared were characterized by attenuated total reflection Fourier transform infrared (ATR-FTIR), solid-state nuclear magnetic resonance (NMR) and X-ray photoelectron (XPS) spectroscopy; these results indicated that by covalent bonding with EDA, the unstable carboxylic groups on the initially generated poly(amic acid) (PAA) TFC membrane surfaces were effectively transformed into polyamide, including the methylene group in the chemical structure chain, for preparing the PAA-cov-EDA NF membranes. At an operating pressure of 1.0 MPa, the PAA-cov-EDA NF membrane exhibits a glucose rejection of 90% at a flux of 25 L $m^{-2}$ $h^{-1}$, and a $MgSO_4$ rejection of 76% at the flux of 31 L $m^{-2}$ $h^{-1}$, in particular demonstrating superior chlorine resistance, after being immersed in a 200 ppm NaClO solution for 100 h. Such novel polyamide TFC NF membranes have advantages of mild preparation conditions and high rejection towards low-molecular-weight organics, thus demonstrating potential in the pharmaceutical industry.

Received 00th January 2012,
Accepted 00th January 2012

DOI: 10.1039/x0xx00000x

www.rsc.org/MaterialsA

## 1 Introduction

Nanofiltration (NF) with advantages of low operation pressure and energy consumption is a pressure-driven membrane filtration process between ultrafiltration and reverse osmosis (RO).[1,2] NF has attracted worldwide attention for the production of drinking water and treatment of waste water,[3-7] in particular, it has been utilized for the elimination of low-molecular-weight pharmaceutical residues ranging from 200 to 400.[8-11]

Most NF membranes have the thin film composite (TFC) structure generated by the interfacial polymerization on porous supports.[12,13] Previous studies have reported that the top layers of TFC membranes have different chemical compositions, such as aromatic polyamide,[14,15] cellulose acetate,[16] and poly(vinyl alcohol).[17] The most popular aromatic polyamide thin film has been synthesized by the interfacial polymerization of trimesoyl chloride (TMC) and m-phenylenediamine (MPD). As compared with the TMC synthesized by 1,3,5-benzenetricarboxylic acid, 1,2,4,5-benzene tetracarbonyl chloride (BTC) synthesized by pyromellitic dianhydride is more convenient. By the interfacial polymerization of BTC and MPD, poly(amic acid) (PAA) TFC membranes can be prepared. However, such membranes have *o*-carboxylic acid groups on their surface, which are unstable in the presence of water and tend to form *o*-phthalic acid.[18-21] Generally, thermal imidization is employed to transform PAA TFC membranes into stable polyimide membranes, and such polyimide membranes have been used for RO or gas separation. For instance, Kwon et al.[18] have synthesized PAA TFC membranes using BTC and MPD monomers, followed by thermal treatment at 180 °C for preparing a polyimide RO membrane; Chern et al.[22] have prepared TFC membranes by the interfacial polymerization of BTC and 4,4'-methylene dianiline, followed by thermal treatment at 135 °C for preparing a $CO_2$ separation membrane. Notably, during thermal imidization, shrinking of the polymer membrane and collapse of its porous structure can probably occur.[19,23] Hence, it is intriguing to explore new facile methods, rather than thermal imidization, to easily transform PAA TFC membranes into a stable chemical structure for NF separation.

Considering the chemical transformation of the unstable *o*-carboxylic acid group, some approaches, besides direct thermal imidization, have been reported to improve membrane functionality through chemical interactions with organic amines.[24] For example, Tiraferri et al.[25] have utilized 1-ethyl-3-(3-dimethylaminopropyl) carbodiimide hydrochloride (EDC) and N-hydroxysuccinimide (NHS) to activate the covalent bonding of one terminal of the diamine onto the surfaces of polyamide membranes, while the other free amine terminal was utilized to bind to single-walled carbon nanotubes for improving the antimicrobial property of membrane surfaces. Xu et al.[26] have also utilized amine as the cross-linker for grafting imidazolidinyl urea on a polyamide membrane to improve the anti-biofouling and chlorine resistance properties. These results have inspired us to investigate a diamine-modified method to effectively convert the carboxylic groups on the PAA TFC membranes into amide groups so as to improve the stability of the NF membranes.

On the other hand, the chlorine resistance of composite membranes is one of important factors associated with chemical cleaning in separation processes.[2] Polyamide membranes have been reported to be susceptible to attack by Cl via the N or O atom of the amide groups resulting in the formation of N-chloroamide.[27,28] For instance, Matsuyama et al.[29] have prepared polyamide membranes using MPD and a mixture of TMC and isophthaloyl dichloride and observed that such polyamide membranes exhibited a significant decrease towards NaCl rejection (from 99 to 10%) after the membrane was immersed in a 200 ppm NaClO aqueous solution for 40 h. Konagaya et al.[30] have studied the chlorine resistance of certain polyamides and concluded that aliphatic diamine compounds with a short methylene chain between terminal amine groups improve chlorine resistance.

To transform PAA TFC membrane into a stable chemical structure by non-thermal treatment as well as improve the chlorine resistance of the membrane, in this article, we first prepared PAA TFC membranes on a porous polyetherimide (PEI) support membrane and then studied the effects of two treatment methods using ethylenediamine (EDA) on the separation performance as well as the chlorine resistance property. The TFC NF membranes thus prepared were characterized by attenuated total reflection Fourier transform infrared (ATR-FTIR) as well as solid-state nuclear magnetic resonance (NMR) spectroscopy, and X-ray photoelectron spectroscopy (XPS), scanning electron microscopy (SEM), atomic force microscopy (AFM) as well as contact angle and zeta potential measurement; from the results obtained, by employing different modification treatments by EDA, the carboxylic groups on the PAA TFC membrane surfaces form interactive bonds with diamine via electrostatic interactions or generate covalent bonds with amine groups. In particular, the covalently modified EDA NF membrane, prepared using BTC and MPD monomers, exhibits glucose rejection higher than 90% and a flux of 25 L $m^{-2}$ $h^{-1}$ at 1.0 MPa as well as superior chlorine resistance.

## 2 Experimental

### 2.1 Chemicals

Polyetherimide (PEI, Ultem 1000) was purchased from Saudi Basic Industries Corporation (Riyadh, Saudi Arabia) and dried at 150 $^{o}$C for 5 h before use. BTC was synthesized using pyromellitic dianhydride and phosphoric chloride according to the previous procedure.[18,31] Polyvinylpyrrolidone (PVP, K30), sodium dodecyl sulfate (SDS), monobasic sodium phosphate, dibasic sodium phosphate, phosphoric acid, EDA, dimethylacetamide (DMAc), n-hexane and the sodium hypochlorite solution (NaClO) were purchased from Tianjin Guangfu Fine Chemical Research Institute (Tianjin, China). EDC and NHS were purchased from Aladdin Reagent Co., Ltd. (Shanghai, China). MPD, glucose and inorganic salts such as NaCl, $MgCl_2$, $MgSO_4$, and $Na_2SO_4$ were purchased from Sinopharm Chemical Reagent Co., Ltd. (Shanghai, China). All chemicals were of analytical grade and used without further purification. Deionized (DI) water was used throughout the study.

### 2.2 Preparation of composite membranes

#### 2.2.1 Preparation of PEI support

The microporous PEI support membrane was prepared by casting a 25 wt% PEI solution in DMAc containing 2 wt% PVP onto a polypropylene non-woven fabric (average pore diameter is 1 μm, purchased from Tianjin TEDA Co., Ltd. China) with a knife gap of 200 μm at room temperature and immersing into a water coagulation bath for 60 min. The PEI support thus obtained membrane was thoroughly washed using DI water.

#### 2.2.2 Preparation of composite NF membranes

As shown in scheme 1, three composite NF membranes were prepared by the interfacial polymerization of BTC and MPD on the surface of the PEI support membranes.

The first NF membrane is the unmodified TFC membrane: First, an aqueous solution containing MPD (2 wt%) and SDS (0.15 wt%) was poured over the PEI support membranes at room temperature; second, after 2 min, the excess solution was removed. Subsequently, a hexane solution of 0.1 wt% BTC was poured on the saturated membrane for 2 min to generate the PAA thin film over the PEI support by polymerization. Finally, the obtained composite NF membranes were dried in air for 15 min. Hereafter, this PAA TFC membrane will be referred to as unmodified PAA.

In the second NF membrane, the carboxylic acid groups are linked to the amine by electrostatic interactions. Considering that the carboxylic acid groups on the surface are susceptible to reaction with amine, the prepared PAA TFC membrane was then immersed in an aqueous solution of 5 wt% EDA for 5 min. After washing using DI water, the modified membrane, denoted as PAA-ion-EDA, was assessed by NF separation experiments.

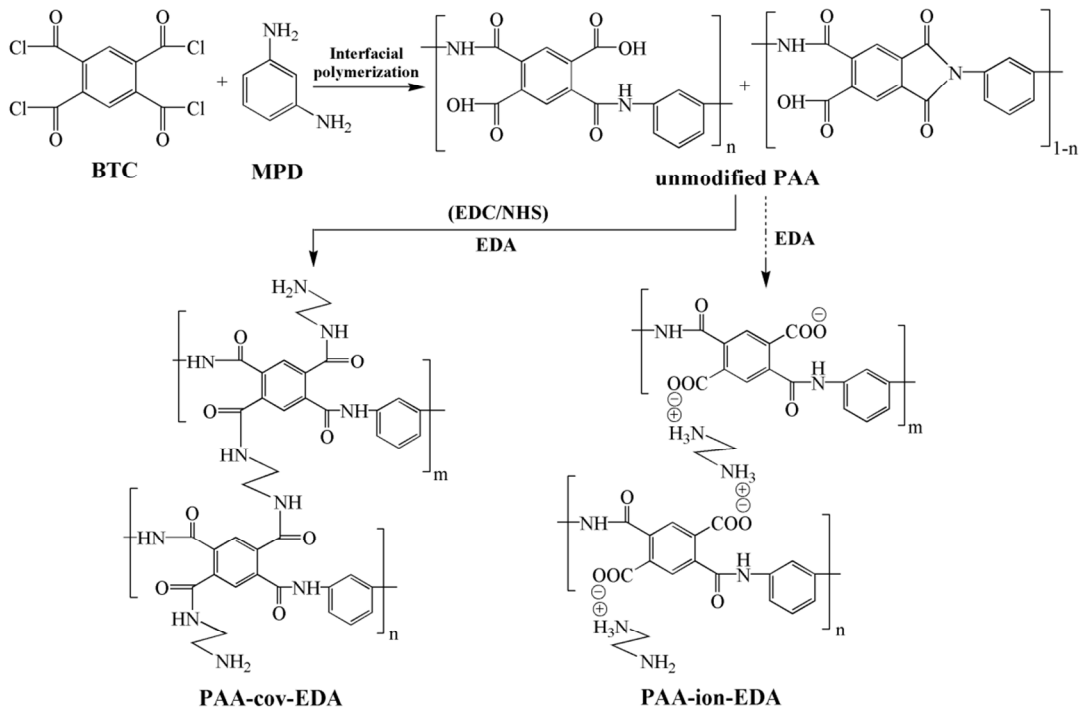


**Scheme 1.** Preparation of three NF membranes: unmodified PAA, PAA-ion-EDA and PAA-cov-EDA

The third NF membrane, denoted as PAA-cov-EDA, is another modified PAA TFC membrane, where the carboxylic acid groups on the PAA TFC membrane surface are covalently linked with amine. The PAA-cov-EDA was prepared by first immersing unmodified PAA membrane in an aqueous solution of 6 wt% EDC at room temperature for 10 min; second, NHS was quantitatively added into this solution with an NHS/EDC mass ratio of 0.5 for activating the carboxylic acid groups on the membrane surface. Next, after 10 min, an aqueous solution of 5 wt% EDA was added, and the mixture was kept aside in a dark place for 12 h for generating stable covalent bonds between the carboxylic acid group and amine group of EDA. PAA-cov-EDA thus obtained was washed using DI water before the assessment of NF experiments.

### 2.3 Membrane characterization

#### 2.3.1 Spectral analysis

The structure of the membranes was characterized by ATR-FTIR spectroscopy (Bio-Rad, FTS-6000) using a zinc selenide crystal at a 45° angle of incidence. The structure of the top layers of membranes was characterized by the same spectrometer. At least 16 scans were recorded for each spectrum at a resolution of 8.0 $cm^{-1}$.

The individual top layers of unmodified PAA, PAA-ion-EDA and PAA-cov-EDA were prepared in the absence of the PEI support and polypropylene non-woven fabric and characterized by solid-state $^{13}C$ NMR spectroscopy. NMR spectra were recorded on a Varian InfinityPlus 300 MHz spectrophotometer equipped with a 4.0 mm double-tuned probe. NMR experiments were conducted under conditions of magic angle spinning at 10.0 kHz and a 90° pulse of 3.0 μs with a repetition delay of 5 s. Chemical shifts were referenced to the corresponding nuclei in tetramethylsilane.

The chemical compositions of the top thin films of NF membranes were analyzed by XPS (PHI5000VersaProbe, ULVAC-PHI Inc., Osaka, Japan) using AlKα as the radiation source and the spectra were recorded at an electron emission angle of 45°.

#### 2.3.2 Morphology, contact angle and zeta potential measurement

SEM was adopted to observe the surface and cross-section morphologies of the membrane (Hitachi S4800, Japan). To observe the top surface and cross-section morphologies, the membrane samples were sputter-coated with gold before SEM analysis.

Tapping mode AFM was performed for analyzing surface roughness analysis (Agilent 5500, America) in air. All the surface roughness values presented were data obtained from an average of three membrane samples.

The hydrophilicity of the composite membrane surfaces was characterized by static contact angle measurements (JC2000C Contact Angle Meter, Powereach Co., Shanghai, China) at room temperature. At least five water contact angles at different locations on one surface were averaged to obtain a reliable value.

The zeta potential of membranes was measured using an electrokinetic analyzer (Anton Paar GmbH, Austria); these measurements were conducted in a background electrolyte solution containing 10 mM KCl over a pH range of 3-7 at 25 °C. The resultant zeta potential was calculated from the Helmholtz-Smoluchowski equation.

### 2.3.3 Separation performance tests

Permeation tests were conducted using a cross-flow membrane separation system, with the diameter of a circular membrane being 8 cm. Feed streams for the rejection and solution flux experiments were prepared by dissolving glucose in DI water (pH=5.9) or in phosphate buffers at pH 3.2 and 7.2, respectively.[32] The initial glucose concentration in feed streams was 10 g/L. The rejection and flux of inorganic salts were obtained with 2 g/L of NaCl, $MgCl_2$, $MgSO_4$ and $Na_2SO_4$ in DI water (pH=5.9). All separation experiments were performed at an operation pressure of 1.0 MPa and a temperature of 25 °C with at least three repetitions. The glucose concentration was measured using an Agilent Technologies 1200 series HPLC equipped with a 4.6mm ID×150 mm column maintained at 30 °C. The mobile phase was 75:25 acetonitrile-water, injection volume was 30 μL, and flow rate was 1.4 mL/min. The concentrations of inorganic salt aqueous solutions were measured by electrical conductivity (DDS-307, Shanghai Shengci Instrument Co., Ltd. China).

Flux ($F$) was determined by measuring the permeate volume ($V$) per unit area ($A$) per unit time ($t$) according to equation (1).

$$F = \frac{V}{A \times t} \quad (1)$$

Rejection ($R$) was calculated using equation (2), where $C_P$ and $C_f$ are the solute concentrations in the permeate and feed solution, respectively.

$$R = (1 - \frac{C_p}{C_f}) \times 100\% \quad (2)$$

### 2.3.4 Chlorine resistance of composite NF membrane

To evaluate the chlorine resistance property, the composite NF membranes were first immersed in an aqueous solution of 200 ppm NaClO at different times and then rinsed with pure water to measure their separation performance. The flux and rejection of glucose and salt solutions were measured and calculated as above.

## 3 Results and discussion

### 3.1 ATR-FTIR spectra

To investigate the variation in the structures of the three NF membranes as compared to the structure of the PEI support, ATR-FTIR spectra were recorded. As shown in Fig. 1(a), for the PEI support, major bands are observed at 2963 $cm^{-1}$ and 1720 $cm^{-1}$, which are attributed to aliphatic C-H bands and imide C=O stretching vibration of PEI, respectively, together with a band at 1681 $cm^{-1}$, which are attributed to the carbonyl of PVP. For unmodified PAA, two bands are observed at 1656 $cm^{-1}$ and 1545 $cm^{-1}$, which are attributed to C=O stretching (amide I) and N-H stretching (amide II), respectively, whereas the bands corresponding to the PEI support at 2963 $cm^{-1}$ and 1681 $cm^{-1}$ disappear, together with the weakening of the band at 1720 $cm^{-1}$. For PAA-ion-EDA and PAA-cov-EDA NF membranes, a small broad band is observed at 3230 $cm^{-1}$, which is attributed to the amine NH stretching of EDA. Another band is observed at 1600 $cm^{-1}$, which is attributed to the breathing of the aromatic ring; meanwhile, the relative intensity of the amide II band at 1545 $cm^{-1}$ increases. The values of the band intensity ratio, $I_{1545}/I_{1600}$, are calculated as 0.78, 0.77 and 0.95 for unmodified PAA, PAA-ion-EDA and PAA-cov-EDA, respectively. It is suggested that the structure of the PAA-cov-EDA NF membrane consists of more fractions of amide N-H groups as compared to the unmodified PAA and PAA-ion-EDA NF membranes.

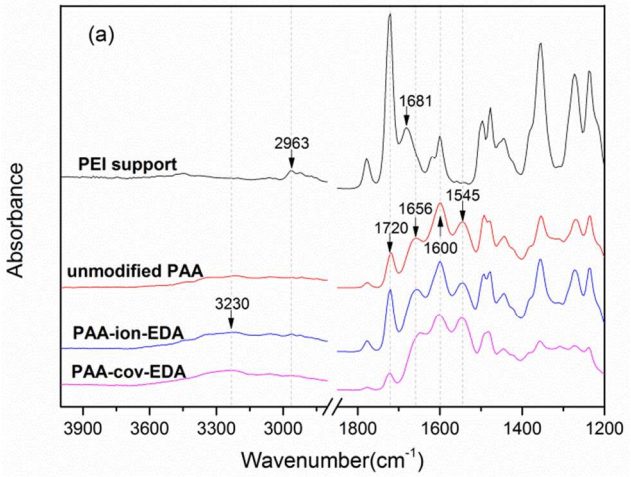


**Fig. 1(a).** ATR-FTIR spectra of the PEI support, unmodified PAA, PAA-ion-EDA and PAA-cov-EDA membranes.

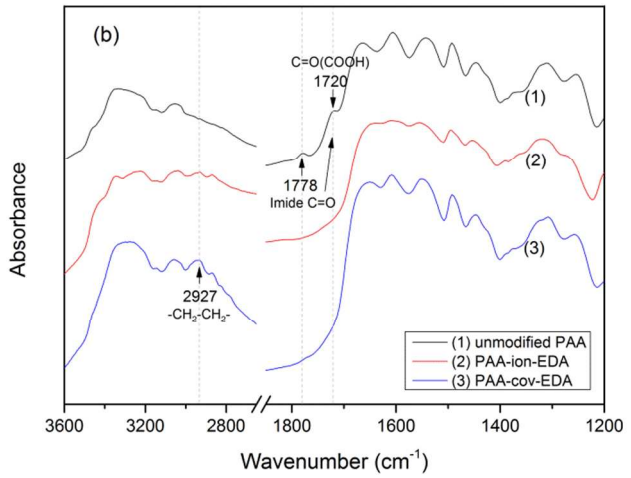


**Fig. 1(b).** FTIR spectra of the top layers of unmodified PAA, PAA-ion-EDA and PAA-cov-EDA membranes.

Further, the top layers of unmodified PAA, PAA-ion-EDA and PAA-cov-EDA were prepared without the membrane support and characterized by FTIR. As shown in Fig. 1(b), for unmodified PAA, two typical bands are observed at 1778 $cm^{-1}$ and 1720 $cm^{-1}$, respectively, which correspond to the imide C=O. Meanwhile, the band at 1720 $cm^{-1}$ is also attributed to the carboxyl C=O. Previous studies have reported that carboxylic acid groups are generated by the interfacial polymerization of BTC and MPD.[18,22] Therefore, the chemical structure of the top layer of unmodified PAA consists of carboxylic acid groups and a small fraction of imide groups, as shown in Scheme 1. In contrast, for the top layers of PAA-ion-EDA and PAA-cov-EDA membranes, no bands are observed at 1720 $cm^{-1}$ and 1778 $cm^{-1}$, indicating the absence of carboxylic acid and imide groups. Meanwhile, for PAA-ion-EDA and PAA-cov-EDA, clear bands are observed at 2927 $cm^{-1}$, which correspond to the $-CH_2-CH_2-$ stretching vibration. It is confirmed that by the following modification, the diamine groups of EDA indeed react with the carboxylic acid and imide groups on the surface of the unmodified PAA membrane.

### 3.2 Solid-state $^{13}C$ NMR spectra

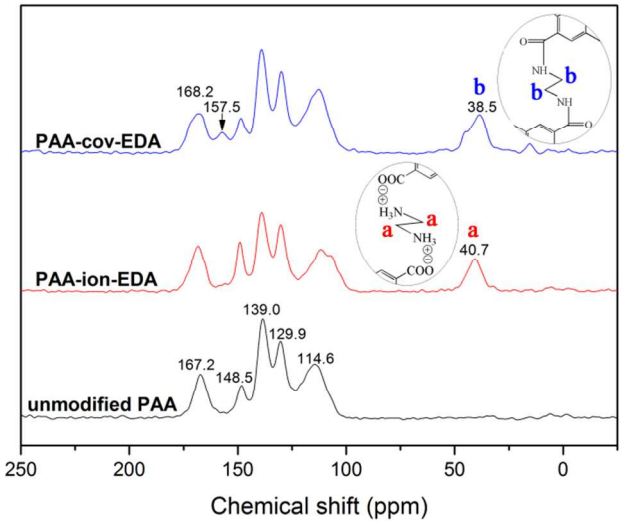


**Fig. 2.** Solid-state $^{13}C$ NMR spectra for the top layers of unmodified PAA, PAA-ion-EDA and PAA-cov-EDA membranes.

Solid-state $^{13}C$ NMR spectroscopy was performed to distinguish in detail the chemical structure differences among the top layers of three NF membranes. For the top layer of the unmodified PAA membrane, as shown in Fig. 2, a peak is observed at 167.2 ppm, which corresponds to the acid and amide carbonyl carbon; also, four distinct signals are observed at 148.5, 139.0, 129.9 and 114.6 ppm, corresponding to the aromatic carbons.[33,34] After modification with EDA, a peak is observed at 40.7 ppm, corresponding to the carbon atoms in the methylene (labelled by 'a') in PAA-ion-EDA. On the other hand, for the top layer of the PAA-cov-EDA membrane, the carbonyl carbon peak shifts to 168.2 ppm, and a peak is observed at 38.5 ppm, corresponding to the methylene carbon (labelled by 'b') in PAA-cov-EDA, together with a new small peak at 157.5 ppm. These results suggest that in the PAA-cov-EDA membrane, the carboxylic acid groups react with diamine to form covalently linked bonds.

### 3.3 XPS spectra

XPS spectra of the three NF membranes were recorded to characterize the elemental compositions and species of nitrogen and oxygen in the top films of the three membranes. As listed in Table 1, unmodified PAA consists of 76.0% carbon, 13.3% nitrogen and 10.7% oxygen, while for the PAA-ion-EDA and PAA-cov-EDA NF membranes, the carbon content decreases to 73.0% and 71.9%, respectively, together with a marginal increase of nitrogen and oxygen caused by the incorporation of diamine and generated new amide bonds.

**Table 1** Elemental compositions of three NF membranes.

| Membranes | Element content (atom.%) | | |
|---|---|---|---|
| | C | N | O |
| unmodified PAA | 76.0 | 13.3 | 10.7 |
| PAA-ion-EDA | 73.0 | 13.6 | 13.4 |
| PAA-cov-EDA | 71.9 | 16.3 | 11.8 |

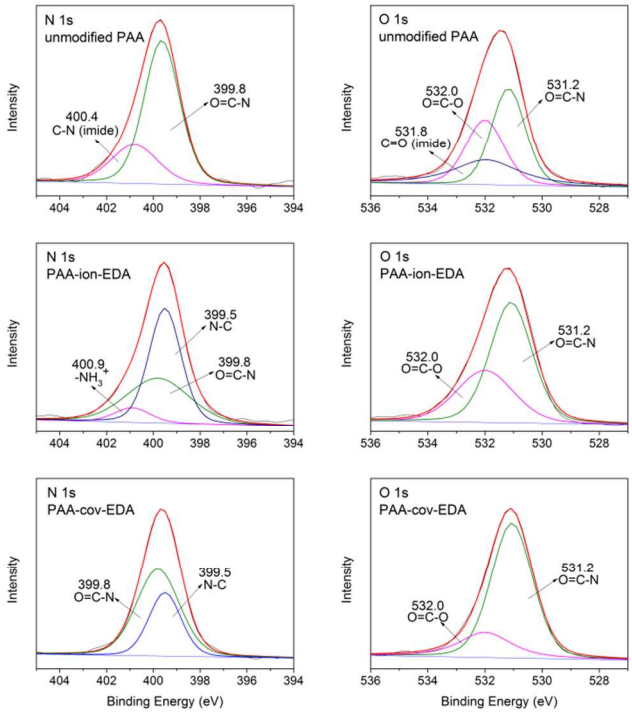


**Fig. 3.** High-resolution nitrogen and oxygen 1s XPS spectra of the unmodified PAA, PAA-ion-EDA and PAA-cov-EDA membranes.

The deconvoluted XPS N1s and O1s spectra of these NF membranes were obtained to discriminate nitrogen and oxygen species (Fig. 3). For unmodified PAA, two nitrogen species are located at 399.8 eV and 400.4 eV, which correspond to the O=C-N bond of the amide and the C-N bond of the imide, respectively. On the other hand, three oxygen species are located at 531.2 eV, 531.8 eV, and 532.0 eV, which correspond

to the O=C-N of amide, C=O of imide and O=C-O of carboxyl acid, respectively. A small fraction of imide bonds is observed in unmodified PAA (Scheme 1), which is consistent with the FTIR results (Fig. 1b).

For PAA-ion-EDA, the nitrogen species are located at 399.5 eV, 399.8 eV, and 400.9 eV, which correspond to the N-C bond, O=C-N bond and $-NH_3^+$, respectively, suggesting the formation of interactive bonding between the carboxylic acid groups on the surface of the PAA membrane and diamine of EDA by electrostatic interactions. For PAA-ion-EDA, the oxygen species are located at 531.2 eV and 532.0 eV, which correspond to the O=C-N of the amide and the O=C-O of the carboxyl, respectively. In combination with $^{13}C$ NMR spectra (Fig. 2), the building block of diamine has been intercalated into the chemical structure of the PAA-ion-EDA membrane through terminals associated with relatively weak interactions between $-COO^-$ and $-NH_3^+$, as shown in Scheme 1. For PAA-cov-EDA, two nitrogen species are observed at 399.5 eV and 399.8 eV, which correspond to the N-C bond of the aliphatic diamine and the O=C-N bond of the amide, respectively. Meanwhile, in the XPS O1s spectra, major and minor peaks are observed at 531.2 eV and 532.0 eV, corresponding to the amide oxygen and carboxylic oxygen, respectively. It is indicated that the PAA-cov-EDA membrane consists of the covalent bonds between the carboxylic groups and diamine of EDA.

### 3.4 Surface morphology, hydrophilicity and charge analysis

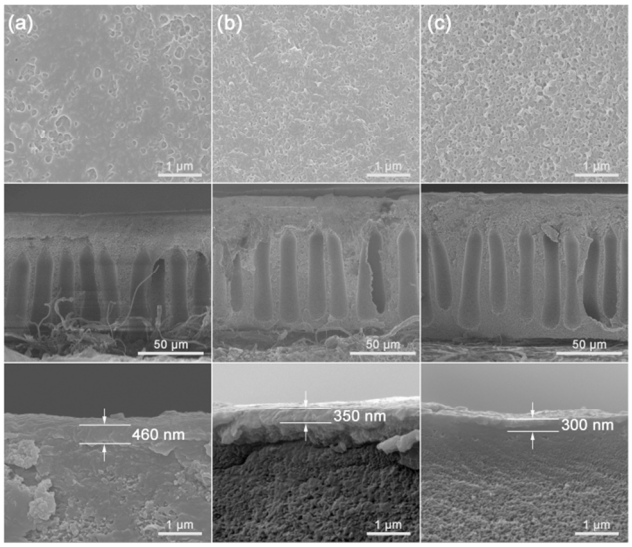


**Fig. 4.** SEM images of the top surface and cross-sections of the NF membranes of unmodified PAA (a), PAA-ion-EDA (b) and PAA-cov-EDA (c).

Fig. 4 shows the SEM images of the three NF membranes. As shown in Fig. 4a, the top surface of the unmodified PAA membrane is tight and rough. After modification with EDA, the surfaces of the PAA-ion-EDA (Fig. 4b) and PAA-cov-EDA (Fig. 4c) membranes become uniform and smooth with "ridge and valley type" structures. Meanwhile, the cross-sections of three NF membranes exhibit an asymmetric structure, which is composed of a top skin layer and a finger-like porous support layer, as a result of strong affinity between solvent and water in the coagulation bath.[35] The thickness of the top skin layer decreases in the order: 460 nm (unmodified PAA) > 350 nm (PAA-ion-EDA) > 300 nm (PAA-cov-EDA). As shown in Scheme 1, by modification with EDA, the diamine groups of EDA react with the carboxylic acid and imide groups on the surface of the unmodified PAA membrane. Consequently, the chemical structures of the top layers of PAA-ion-EDA and PAA-cov-EDA membranes are composed of high amounts of cross-linked parts rather than linear parts, which results in the lower thickness of the top layer. It is clear that the modification with EDA results in the changes of both chemical groups and structures of the top skin layers of NF membranes.

AFM analysis was conducted for further investigation of the surface morphology of NF membranes. Fig. 5 shows the three-dimensional AFM images of the unmodified PAA, PAA-ion-EDA and PAA-cov-EDA membranes. The root mean square roughness (Rms) values of the membrane surface are 50.3 ± 5.7 nm, 32.0 ± 1.5 nm and 40.3 ± 4.8 nm for unmodified PAA, PAA-ion-EDA and PAA-cov-EDA, respectively. These results indicate that modification with EDA makes the membrane surface smooth.

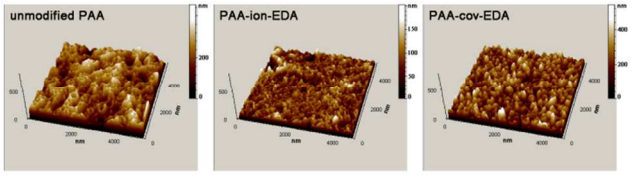


| Membranes | Rms (nm) | Ra (nm) |
|---|---|---|
| unmodified PAA | 50.3 ± 5.7 | 38.6 ± 4.5 |
| PAA-ion-EDA | 32.0 ± 1.5 | 25.4 ± 1.9 |
| PAA-cov-EDA | 40.3 ± 4.8 | 31.9 ± 3.8 |

**Fig. 5.** Three-dimensional AFM images (including morphological statistics) of unmodified PAA, PAA-ion-EDA and PAA-cov-EDA membranes.

Water contact angles are measured to assess the hydrophilicity of the three NF membranes. As listed in Table 2, the average contact angles are 55.3 ± 1.6°, 45.8 ± 2.9° and 42.8 ± 2.5° of the unmodified PAA, PAA-ion-EDA and PAA-cov-EDA, respectively, suggesting that the hydrophilicity of NF membranes is improved after modification with EDA.

**Table 2** Water contact angles on the unmodified PAA, PAA-ion-EDA and PAA-cov-EDA NF membranes.

| Membranes | Contact angle (°) |
|---|---|
| unmodified PAA | 55.3 ± 1.6 |
| PAA-ion-EDA | 45.8 ± 2.9 |
| PAA-cov-EDA | 42.8 ± 2.5 |

Fig. 6 shows the zeta potentials of the unmodified PAA, PAA-ion-EDA and PAA-cov-EDA NF membranes as a function of pH. For unmodified PAA, the isoelectric point is located at pH 3.2, while it shifts to pH 4.6 for the PAA-ion-EDA and PAA-cov-EDA NF membranes. The negative zeta

potential is due to the dissociation of the carboxylic acid groups on the membrane surface, while the positive zeta potential is attributed to the protonation of amine groups. For PAA-ion-EDA and PAA-cov-EDA, the shifts of the isoelectric point suggest that the amount of carboxylic acid groups on the membrane surfaces obviously decreases after modification with EDA. Notably, the zeta potentials of the PAA-ion-EDA membrane in the presence of electrolytes such as $Na_2SO_4$, $MgSO_4$, and $MgCl_2$ must be different from those measured in KCl, owing to the susceptibility of the electrostatically linked terminals between $–COO^-$ and $–NH_3^+$ to divalent ions (Figs. 2 and 3).

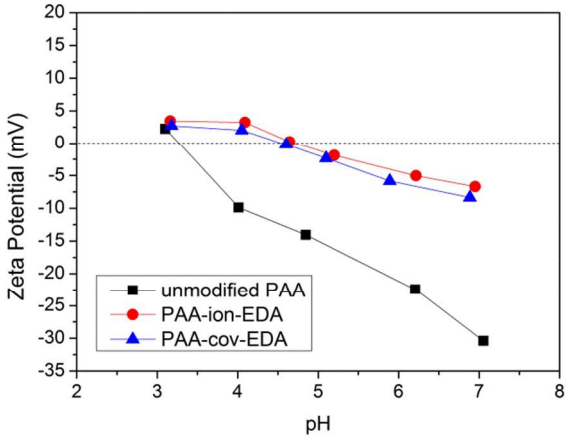


**Fig. 6.** Zeta potentials of the unmodified PAA, PAA-ion-EDA and PAA-cov-EDA NF membranes at different pH values.

### 3.5 Permeation performance

Fig. 7 shows the flux and rejection of the three NF membranes for an aqueous glucose solution with a pH of 5.9. The unmodified PAA NF membrane exhibits a flux of 4.5 L $m^{-2}$ $h^{-1}$ and a rejection of 100% towards glucose, while the EDA-modified NF membranes exhibit a higher flux. PAA-ion-EDA exhibits a flux of approximately 20 L $m^{-2}$ $h^{-1}$ and a glucose rejection of approximately 95%, whereas PAA-cov-EDA exhibits a flux of 25 L $m^{-2}$ $h^{-1}$ and a rejection of 90%. By combining the results obtained from the water contact angles and SEM images of these NF membranes, modification with EDA is observed to not only improve the hydrophilicity of the membrane surface but also change the structures of the top skin layers of the PAA NF membranes, resulting in a significant increase in the flux while maintaining a good rejection (>90%) towards low-molecular-weight glucose (MW=180).

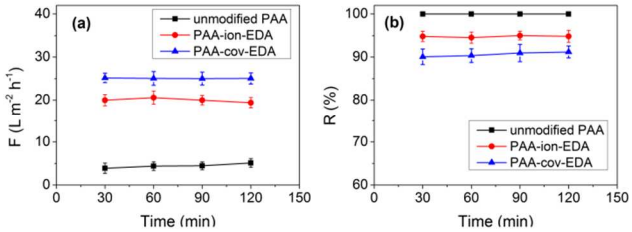


**Fig. 7.** Flux (a) and rejection (b) of unmodified PAA, PAA-ion-EDA and PAA-cov-EDA NF membranes for the aqueous glucose solution (pH 5.9) at 1.0 MPa.

Taking into account the zeta potential variation of these NF membranes, the effect of pH on the flux and rejection towards glucose was investigated. As shown in Fig. 8, as the pH of the feed solution increases from 3.2 to 7.2, for the PAA-ion-EDA NF membrane, the flux increases from 14 to 23 L $m^{-2}$ $h^{-1}$, while the rejection of glucose increases from 94% to 98% with a run time of 120 min, indicating the monotonic increase of both flux and rejection with the pH of the feed solution. For the PAA-cov-EDA NF membrane, as shown in Fig. 9, the flux is approximately 25 L $m^{-2}$ $h^{-1}$ regardless of the pH, while the rejection reaches the maximum (90%) at pH 5.9 followed by 86% at pH 7.2 and 78% at pH 3.2.

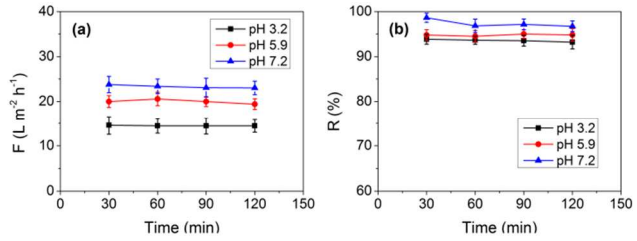


**Fig. 8.** Flux (a) and rejection (b) of the PAA-ion-EDA membrane for an aqueous glucose solution at pH of 3.2, 5.9 and 7.2 at 1.0 MPa.

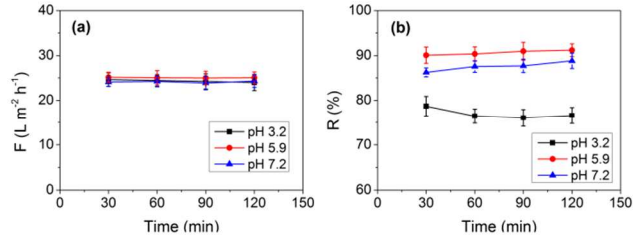


**Fig. 9.** Flux (a) and rejection (b) of the PAA-cov-EDA membrane for an aqueous glucose solution at pH of 3.2, 5.9 and 7.2 at 1.0 MPa.

According to the zeta potential values, the amine groups of the PAA-ion-EDA membrane are protonated at pH 3.2 and the positive charges repel each other, leading to the narrowing of membrane pores and a reduction in the flux.[32] For the PAA-cov-EDA membrane, glucose rejection decreases to less than 80% at pH 3.2 (Fig. 9b), which is probably caused by the conformation change around the amine groups of covalently grafted EDA so as to generate larger pore structures.

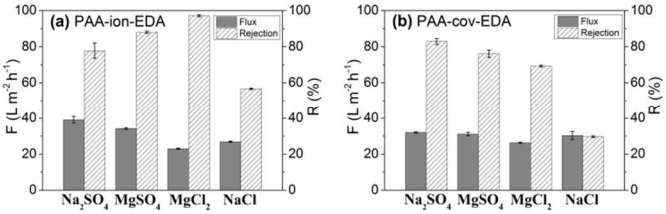


**Fig. 10.** Flux and rejection of the PAA-ion-EDA (a) and PAA-cov-EDA (b) NF membranes for an aqueous solution of inorganic salts at 1.0 MPa.

The performance of the PAA-ion-EDA and PAA-cov-EDA NF membranes was further assessed for aqueous solutions of inorganic salts such as NaCl, $MgCl_2$, $MgSO_4$ and $Na_2SO_4$. As

shown in Fig. 10(a), the flux of the PAA-ion-EDA NF membranes is highly dependent on the salt species. For instance, the flux values are approximately 39 L $m^{-2}$ $h^{-1}$, 34 L $m^{-2}$ $h^{-1}$, 27 L $m^{-2}$ $h^{-1}$ and 23 L $m^{-2}$ $h^{-1}$ for $Na_2SO_4$, $MgSO_4$, NaCl and $MgCl_2$ solutions, respectively. On the other hand, rejection decreases in the order of $MgCl_2$ (97%) > $MgSO_4$ (88%) > $Na_2SO_4$ (78%) > NaCl (57%).

Previous studies[36,37] have indicated that cationic membranes exhibit higher rejection towards $MgCl_2$ than $Na_2SO_4$ caused by the Donnan exclusion, and divalent counter-ions such as $SO_4^{2-}$ can significantly affect the electric field of membranes so as to weaken the Donnan effect; thus, rejection of $MgCl_2$ is higher than that of $MgSO_4$. The higher $MgSO_4$ rejection as compared with that of $Na_2SO_4$ is attributed to the larger size of hydrated $Mg^{2+}$. Combining with the separation performance of PAA-ion-EDA, it is reasonable to conclude that the PAA-ion-EDA membrane is positively charged in the presence of electrolytes such as $Na_2SO_4$, $MgSO_4$ and $MgCl_2$, owing to the existence of electrostatically linked terminals between $–COO^-$ and $–NH_3^+$. Because the sulfate salts in aqueous solutions can interact with the electrostatically linked terminals, the free volumes of the PAA-ion-EDA membrane become larger, resulting in higher fluxes for $Na_2SO_4$ and $MgSO_4$ aqueous solutions. Meanwhile, it is suggested that the chemical structure of the PAA-ion-EDA membrane is not very stable in the presence of electrolytes with divalent ions.

In the case of the PAA-cov-EDA NF membranes (Fig. 10b), the flux shows a small variation associated with salt species, and decreases in the order of $Na_2SO_4$ (32 L $m^{-2}$ $h^{-1}$) > $MgSO_4$ (31 L $m^{-2}$ $h^{-1}$) > NaCl (30 L $m^{-2}$ $h^{-1}$) > $MgCl_2$ (26 L $m^{-2}$ $h^{-1}$), while rejection changes in the order of $Na_2SO_4$ (83%) > $MgSO_4$ (76%) > $MgCl_2$ (69%) > NaCl (30%). The permeation performance of PAA-cov-EDA for these inorganic salts indicates a negatively charged surface, which is in accordance with the zeta potentials in Fig.6. Previously, Mohammad et al.[38] have reported that the polyamide DK and cellulose acetate CK membranes exhibit a glucose rejection of 78%-85% with a flux of approximately 7.2-10.8 L $m^{-2}$ $h^{-1}$ at 0.2-0.3 MPa. Wickramasinghe et al.[39] have prepared a poly(acrylic acid) grafted NF 270 membrane, which exhibits a flux of 19, 18 and 16 L $m^{-2}$ $h^{-1}$ at 0.3 MPa with glucose rejection of 42%, 60% and 65% at pH 3.15, 6.05 and 7.25, respectively. De et al.[40] have prepared a negatively charged polysulfone NF membrane, which exhibits a glucose rejection of 90% with a flux of 15 L $m^{-2}$ $h^{-1}$ at 0.69 MPa, with the decrease in the rejection towards different salts in the order of $Na_2SO_4$ (52%) > NaCl (40%) > $MgSO_4$ (10%) > $MgCl_2$ (8%) while the flux is approximately 19-22 L $m^{-2}$ $h^{-1}$ at 0.69 MPa. Cao et al.[36] have prepared a positively charged polysulfone NF membrane, which exhibits a flux of 17 L $m^{-2}$ $h^{-1}$ at 0.6 MPa and $MgCl_2$ rejection of 86%, with the rejection to different salts following the order of $MgCl_2$ > $MgSO_4$ > $Na_2SO_4$ > NaCl. Thus, the separation performance of PAA-cov-EDA NF membranes, prepared by the interfacial polymerization of BTC and MPD followed by modification with EDA, is comparable with those reported for other NF membranes, especially with advantages of mild preparation conditions and high rejection towards low-molecular-weight organics, demonstrating potential for applications in the pharmaceutical industry.

### 3.6 Chlorine resistance of NF membranes

The separation performance of the PAA-cov-EDA NF membrane was measured after immersing the membrane in a 200 ppm NaClO solution at different times for evaluating the chlorine resistance of the covalently linked composite NF membrane. As shown in Fig. 11, for the separation of glucose, the flux is maintained at 25 L $m^{-2}$ $h^{-1}$, and glucose rejection is 90% within 100 h, while for the $Na_2SO_4$ aqueous solution, the flux and rejection are stable at 32 L $m^{-2}$ $h^{-1}$ and 83%, respectively, within 100 h. Hence, the PAA-cov-EDA NF membrane has superior chlorine resistance. In combination with the above characterizations, the good chlorine resistance of PAA-cov-EDA NF membrane is attributed to the introduction of the methylene group of EDA into the structure of the polyamide membrane.

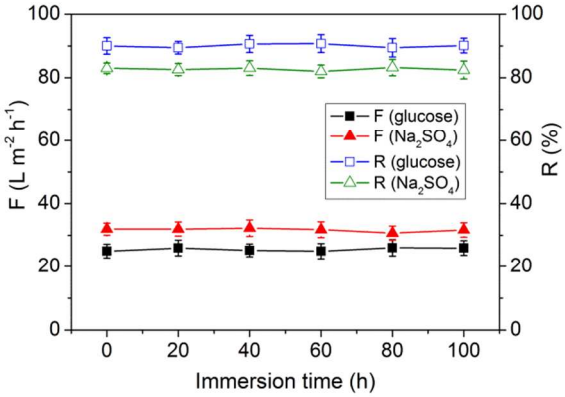


**Fig. 11.** Flux and rejection of the PAA-cov-EDA NF membrane for aqueous solutions of glucose and $Na_2SO_4$ after immersing the membrane in a 200 ppm NaClO solution at 1.0 MPa.

## 4 Conclusions

Novel polyamide thin film composite (TFC) nanofiltration (NF) membranes were prepared on polyetherimide supports by the interfacial polymerization of 1,2,4,5-benzene tetracarbonyl chloride and m-phenylenediamine followed by modification with ethylenediamine (EDA). The TFC NF membranes were characterized by ATR-FTIR and solid-state $^{13}C$ NMR spectroscopy as well as XPS analysis; these results showed that by modification with EDA, the carboxylic groups on the TFC membrane surfaces form interactive bonds with diamine via electrostatic interactions or generate covalent bonds with amine groups. The two polyamide TFC NF membranes, PAA-ion-EDA and PAA-cov-EDA, thus prepared exhibit lower thickness and roughness of the top skin layers. The PAA-ion-EDA NF membrane exhibits a glucose rejection of 95% at a flux of 20 L $m^{-2}$ $h^{-1}$, and a $MgSO_4$ rejection of 88% at a flux of 34 L $m^{-2}$ $h^{-1}$ at an operating pressure of 1.0 MPa. However, owing to the existence of electrostatically linked terminals between $–COO^-$ and $–NH_3^+$, the chemical structure of the PAA-ion-EDA

membrane is not very stable in the presence of electrolytes with divalent ions.

On the other hand, for the PAA-cov-EDA NF membrane, the polyamide TFC membrane including the methylene group in the chemical structure chain exhibits a glucose rejection of 90% at a flux of 25 L $m^{-2}$ $h^{-1}$, and a $MgSO_4$ rejection of 76% at the flux of 31 L $m^{-2}$ $h^{-1}$ at an operating pressure of 1.0 MPa. In particular, the PAA-cov-EDA NF membrane exhibits superior chlorine resistance, showing stable glucose and salt rejection as well as flux after being immersed in a 200 ppm NaClO solution for 100 h. The novel polyamide TFC NF membranes prepared herein have advantages of mild preparation conditions and high rejection towards low-molecular-weight organics, which demonstrate potential for applications in the pharmaceutical industry.

## Acknowledgements

This work was supported by National High-tech R&D Program of China (2012AA03A609). The authors appreciated the help of Dr. Yan Fu (CEEC, Tianjin University) for the detailed discussions on the FTIR analysis.

## Notes and references

Key Laboratory of Systems Bioengineering MOE; Key Laboratory for Green Chemical Technology MOE, Tianjin University; Collaborative Innovation Center of Chemical Science and Chemical Engineering (Tianjin), Tianjin 300072, China.
E-mail: liwei@tju.edu.cn; Fax: +86-22-27890643; Tel: +86-22-27890643

1 Y. Mansourpanah and E. Momeni Habili, *J. Membr. Sci.*, 2013, **430**, 158.
2 R. Han, *J. Membr. Sci.*, 2013, **425-426**, 176.
3 S. Mondal and S. R. Wickramasinghe, *J. Membr. Sci.*, 2008, **322**, 162.
4 R. S. Harisha, K. M. Hosamani, R. S. Keri, S. K. Nataraj and T. M. Aminabhavi, *Desalination*, 2010, **252**, 75.
5 M. Mänttäri, M. Kuosa, J. Kallas and M. Nyström, *J. Membr. Sci.*, 2008, **309**, 112.
6 S. Yu, M. Liu, M. Ma, M. Qi, Z. Lü and C. Gao, *J. Membr. Sci.*, 2010, **350**, 83.
7 A. Y. Zahrim, C. Tizaoui and N. Hilal, *Desalination*, 2011, **266**, 1.
8 W. Zhang, G. H. He, P. Gao and G. H. Chen, *Sep. Purif. Technol.*, 2003, **30**, 27.
9 L. D. Nghiem, A. I. Schafer and M. Elimelech, *Environ. Sci. Technol.*, 2005, **39**, 7698.
10 V. Yangali-Quintanilla, A. Sadmani, M. McConville, M. Kennedy and G. Amy, *Water Res.*, 2009, **43**, 2349.
11 D. Rana, R. M. Narbaitz, A.-M. Garand-Sheridan, A. Westgate, T. Matsuura, S. Tabe and S. Y. Jasim, *J. Mater. Chem. A*, 2014, **2**, 10059.
12 R. J. Petersen, *J. Membr. Sci.*, 1993, **83**, 81.
13 W. J. Lau, A. F. Ismail, N. Misdan and M. A. Kassim, *Desalination*, 2012, **287**, 190.
14 J. Zuo and T.-S. Chung, *J. Mater. Chem. A*, 2013, **1**, 9814.
15 J. E. Gu, S. Lee, C. M. Stafford, J. S. Lee, W. Choi, B. Y. Kim, K. Y. Baek, E. P. Chan, J. Y. Chung, J. Bang and J. H. Lee, *Adv. Mater.*, 2013, **25**, 4778.
16 D. H. N. Perera, S. K. Nataraj, N. M. Thomson, A. Sepe, S. Hüttner, U. Steiner, H. Qiblawey and E. Sivaniah, *J. Membr. Sci.*, 2014, **453**, 212.
17 M. Liu, C. Zhou, B. Dong, Z. Wu, L. Wang, S. Yu and C. Gao, *J. Membr. Sci.*, 2014, **463**, 173.
18 S. Hong, I.-C. Kim, T. Tak and Y.-N. Kwon, *Desalination*, 2013, **309**, 18.
19 C. Ba and J. Economy, *J. Membr. Sci.*, 2010, **363**, 140.
20 M. L. Bender, Y.-L. Chow and F. Chloupek, *J. Am. Chem. Soc.*, 1958, **80**, 5380.
21 J. A. Kreuz, *J. Polym. Sci. Polym. Chem.*, 1990, **28**, 3787.
22 Y.-T. Chern and L.-W. Chen, *J. Appl. Polym. Sci.*, 1992, **44**, 1087.
23 A. Polotsky, V. Cherkasova, I. Potokin, G. Polotskaya and T. Meleshko, *Desalination*, 2006, **200**, 341.
24 P. Nugent, Y. Belmabkhout, S. D. Burd, A. J. Cairns, R. Luebke, K. Forrest, T. Pham, S. Ma, B. Space, L. Wojtas, M. Eddaoudi and M. J. Zaworotko, *Nature*, 2013, **495**, 80.
25 A. Tiraferri, C. D. Vecitis and M. Elimelech, *ACS Appl. Mater. Interfaces*, 2011, **3**, 2869.
26 J. Xu, Z. Wang, L. Yu, J. Wang and S. Wang, *J. Membr. Sci.*, 2013, **435**, 80.
27 J. Glater, S. Hong, M. Elimelech, *Desalination*, 1994, **95**, 325.
28 V. T. Do, C. Y. Tang, M. Reinhard, J. O. Leckie, *Environ. Sci. Technol.*, 2012, **46**, 852.
29 T. Shintani, H. Matsuyama and N. Kurata, *Desalination*, 2007, **207**, 340.
30 S. Konagaya and O. Watanabe, *J. Appl. Polym. Sci.*, 2000, **76**, 201.
31 Y.-T. Chern and L.-W. Chen, *J. Appl. Polym. Sci.*, 1991, **42**, 2543.
32 H. H. Himstedt, K. M. Marshall and S. R. Wickramasinghe, *J. Membr. Sci.*, 2011, **366**, 373.
33 D. T. Padavan, A. M. Hamilton, L. E. Millon, D. R. Boughner and W. Wan, *Acta Biomater.*, 2011, **7**, 258.
34 D. T. Padavan, A. M. Hamilton, D. R. Boughner and W. Wan, *J. Biomater. Sci., Polym. Ed.*, 2011, **22**, 683.
35 W. Chinpa, D. Quémener, E. Bèche, R. Jiraratananon and A. Deratani, *J. Membr. Sci.*, 2010, **365**, 89.
36 X. Li, Y. Cao, H. Yu, G. Kang, X. Jie, Z. Liu and Q. Yuan, *J. Membr. Sci.*, 2014, **466**, 82.
37 W. Fang, L. Shi and R. Wang, *J. Membr. Sci.*, 2014, **468**, 52.
38 A. W. Mohammad, R. K. Basha and C. P. Leo, *J. Food Eng.*, 2010, **97**, 510.
39 H. H. Himstedt, H. Du, K. M. Marshall, S. R. Wickramasinghe and X. Qian, *Ind. Eng. Chem. Res.*, 2013, **52**, 9259.
40 S. R. Panda and S. De, *Desalination*, 2014, **347**, 52.

## Graphical Abstract

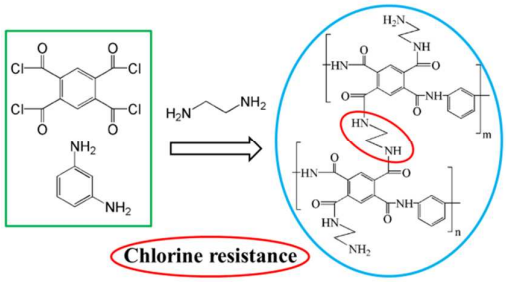


Novel diamine-modified polyamide TFC NF membranes with superior chlorine resistance using BTC and MPD monomers